Communications: SIF Congress 2013

FEL-based wave-mixing spectroscopy at FERMI

F. Bencivenga

Elettra-Sincrotrone Trieste S.C.p.A., AREA Science Park - SS 14 km 163,5
I-34149 Basovizza (TS), Italy

Summary. — I hereby report on the forthcoming development of non-linear co-
herent spectroscopy in the extreme ultraviolet (EUV) and soft x-ray range at the
FERMI free-electron laser (FEL) facility. This class of experiments is routinely used
in the optical domain, where fully coherent photon sources (*i.e.*, lasers) are available.
These methods have not yet developed in the EUV/x-ray range, since photon sources
having characteristics comparable with those of table-top lasers were not available
so far. Such a void is being filled by seeded FELs sources, such as FERMI, which are
in many respects similar to conventional lasers. EUV/soft x-ray non-linear coherent
spectroscopy will be initially focused on the study of collective atomic dynamics in
disordered systems. However, recent advances achieved at FERMI, such as the capa-
bility to radiate multiple and multi-color seeded FEL pulses, opens up the possibility
to largely extend the possible applications of such experimental techniques.

PACS `78.47.jh` – Coherent nonlinear optical spectroscopy.
PACS `41.60.Cr` – Free-electron lasers.

1. – Introduction

The non-linear response of materials is usually described by expanding the polar-
ization of the medium $P(t)$ in powers of the applied electric-field amplitude $E(t)$, *i.e.*:
$P(t) = \epsilon_0[\chi E(t) + \chi^{(2)} E^2(t) + \chi^{(3)} E^3(t) + \ldots]$ [1, 2], where ϵ_0 and χ are the free space
permittivity and the linear susceptibility, respectively, while $\chi^{(n)}$ is a $(n+1)$-order tensor
usually referred to as n-th-order susceptibility. If the non-linear terms of the polarization
are included in Maxwell's equations, then one obtains an inhomogeneous wave equation
in which the non linear-polarization ($P^{NL}(t) = \epsilon_0[\chi^{(2)} E^2(t) + \chi^{(3)} E^3(t) + \ldots]$) acts as
a driving force. $P^{NL}(t)$ can then be regarded as a radiation source, whose frequency
components are not necessarily present in the input fields. Indeed, an n-th-order inter-
action can drive the sample polarization at frequencies given by the sum/difference of

the frequencies contained in the n interacting fields. Such a non-linear mechanism is also referred to as $(n + 1)$-wave-mixing process.

In spite of the conceptual straightforwardness of these first basic steps, non-linear interactions were basically ignored before 1961, when, right after the demonstration of the first laser [3], P. Frenken and coworkers observed the second harmonic generation process, a second-order (three-wave-mixing) process [4]. The coherent nature and high brightness of laser radiation played a key role in the discovery of non-linear wave-mixing processes. Laser devices are indeed able to provide E-values exceeding the ones needed for wave-mixing applications. For instance, given that the order of magnitude for the $\chi^{(n)}$ tensor elements is $\sim E_a^{1-n}$ (where $E_a \sim e/(4\pi\epsilon_0 a_0^2) \approx 5*10^{11}$ V/m is the atomic field strength while a_0 and e are the Bohr radius and the elementary charge, respectively) [1,5], standard table-top lasers can deliver photon pulses with 50 fs duration and 5 mJ pulse energy that, when focused on a $100\,\mu m^2$ spot, lead to an irradiance $I \approx 10^{17}$ W/cm^2 and thus to $E = \sqrt{2I/(\epsilon_0 c)} \approx 8.5*10^{11}$ V/m (being c the speed of light). In such a high field ($E > E_a$) regime the non-linear response is dominating and cannot be treated in a "perturbative approach", $i.e.$ the power series expansion of $P(t)$ does not converge for $E > E_a$. Indeed, wave-mixing experiments are usually carried out at E-values well below E_a. In such a "not-too-high" field regime the coherence of laser radiation is a key requirement for the observation of non-linear wave-mixing signals. This can be understood by considering an isolated dipole illuminated by two electromagnetic fields of frequency ω_1 and ω_2. Non-linear effects force the dipole to oscillate at $\omega_1 + \omega_2$ and, therefore, it can emit radiation at that frequency. Now, if one considers coherent radiation that illuminates a sample containing an ensemble on N dipoles, then all dipoles falling within the coherence volume of the incident fields oscillate in phase, which is determined by the phase of the driving radiation. The $\omega_1 + \omega_2$ fields radiated by the single dipoles then add in amplitude rather than in intensity along the $\vec{k}_1 + \vec{k}_2$ direction; $\vec{k}_{1,2}$ are the wave vectors of the input fields [1, 2]. The latter condition, also termed phase-matching [6], ensures that the intensity of the $\omega_1 + \omega_2$ emission scales as N^2 rather than N, thus enormously enhancing the intensity of the wave-mixing ($\omega_1 + \omega_2$) signal. This may even turn into a macroscopically observable coherent beam propagating after the sample along a well defined direction, given by the phase matching conditions. Such a marked directionality usually implies that, within a small solid angle around the $\vec{k}_1 + \vec{k}_2$ direction, the intensity of the wave-mixing signal largely exceeds the one due to linear interactions, typically featured by more isotropic distributions of the emitted radiation. This feature is routinely used, for instance, in optical coherent Brillouin and Raman scattering methods to greatly improve the signal/noise ratio with respect to the corresponding spontaneous (linear) scattering mechanisms [1, 2, 7, 8].

In these last decades non-linear optics has been applied to several fields, ranging from fundamental studies of radiation-matter interactions [7-9] to technological applications, such as, $e.g.$, quantum communications [10], optical switchers [11] and sub-wavelength resolution imaging [12]. Several experimental methods based on optical wave-mixing are currently used to study dynamics of very different nature ($e.g.$, phonons [7,8], spin waves [13], charge transfer [14], etc.) that occur at very different timescales, ranging from milliseconds [15] to femtoseconds [16]. The broad exploitable timescale range and the large versatility of these methods make wave-mixing based experiments invaluable experimental tools to study dynamics in almost all classes of samples: condensed matter [7,8], nanostructures [17], surfaces [18] or isolated molecules [19].

The last decades have also witnessed an enormous boost of scientific and technological applications based on EUV and x-ray radiation. This was mostly triggered by

the development of third generation synchrotrons. In particular, the high brilliance and wavelength tunability of these sources allowed the development of several core-level spectroscopies, such as resonant inelastic x-ray scattering, anomalous x-ray diffraction, x-ray absorption and emission spectroscopy. These methods are invaluable tools to study the structural and electronic properties of matter at the inter- and intra-molecular scale, and also allow for element and chemical state sensitivity. On the other hand, dynamic information attainable by these techniques are relatively scarce, though pioneering time resolved (pump-probe) studies have been recently carried out by combining synchrotron and laser sources [20-22].

The eventual development of wave-mixing methods in the EUV/x-ray range could represent a fruitful way to obtain information on a broad variety of dynamics, with the additional benefits of element selectivity and few- to sub-nm spatial resolution, capabilities unattainable in the optical domain. In this respect, a major limitation of synchrotron radiation is its essentially incoherent nature. Indeed, the number of photons in each synchrotron pulse that fall within the coherence volume is of the order of unity. In this case the radiation-matter interaction can be described as "one photon at a time" and, therefore, the observed signal can be essentially assumed to be the sum of a certain number of uncorrelated single photon interactions. Conversely, almost all photons emitted by a conventional laser fall within the same coherence volume, so that they can "work together" to stimulate non-linear effects. Coherent EUV/x-ray pulses can be also obtained through high-harmonic-generation processes [23]. However, at the present stage of development, these sources are not able to deliver photon pulses with high enough intensity to stimulate non-linear effects and are also limited in their wavelength tunability.

The recent development of EUV/x-ray FELs allows to overcome the limitations of both synchrotron and high-harmonic-generation sources, since FEL sources can deliver photon pulses with brightness comparable with that of optical lasers and a high degree of transverse coherence [24]. A high degree of longitudinal (time) coherence can be also obtained by exploiting seeding schemes, such as those adopted at LCLS x-ray FEL (Stanford, USA) and at FERMI, the novel XUV/soft x-ray FEL source located at the Elettra-Sincrotrone Trieste facility (Trieste, Italy) [25]. The seeding scheme adopted at FERMI relies upon an external UV laser (λ_{seed} in the 220–300 nm range) that triggers the high-gain-harmonic-generation process [26]. The latter leads to the FEL emission at wavelength $\lambda_{FEL} = \lambda_{seed}/H$, where H is an integer number (usually in the 3–15 range) corresponding to the harmonic at which the FEL is tuned. The fluctuations in the relevant photon parameters (intensity, central wavelength, bandwidth, etc.) are greatly reduced as compared to unseeded FELs and, furthermore, the coherence properties of the seeding pulse are preserved in the FEL output [27]. Seeded FELs may then provide the coherent electromagnetic fields required for EUV/x-ray wave-mixing applications. Indeed, ultrafast FEL pulses with moderate energy (say a few μJ in a few 10's of fs) focused onto a $\approx 1000\,\mu$m^2 spot can provide E-values $\approx 0.02 * E_a$, that are in the range usually employed in optical wave-mixing. Finally, since all photon parameters of the seed laser can be controlled, it is possible to determine the photon output of a seeded FEL by acting on the seed laser. This unique feature can be used, *e.g.*, to easily achieve continuous wavelength tunability [28] or a multi-color FEL emission [29]. In the context of wave-mixing applications these options can be employed (as discussed further below) to provide element and excitation selectivity, thus opening up the unprecedented opportunity to transfer the most advanced table-top optical methods in the EUV/x-ray range.
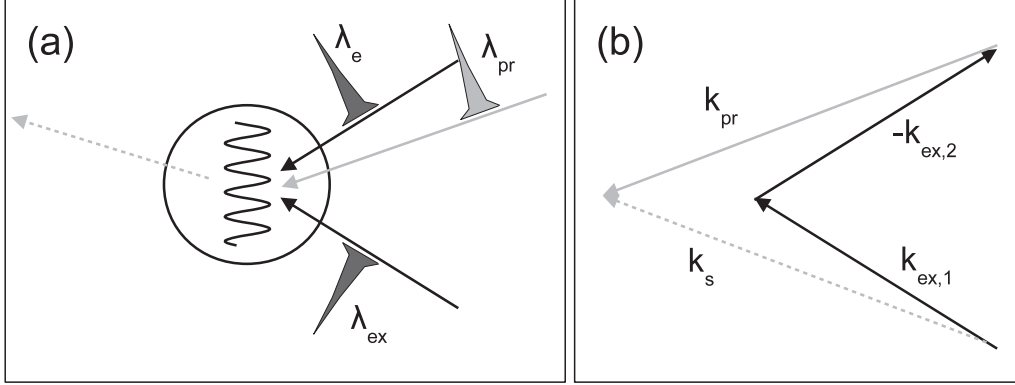
Fig. 1. – (a) Sketch of a TG experiment: black lines are the interfering pump pulses, full and dotted grey lines are the probe and signal beams, respectively. (b) Phase matching condition (Bragg scattering) for the beams shown in panel (a): $\vec{k}_s$, $\vec{k}_{pr}$, $\vec{k}_{ex,1}$ and $\vec{k}_{ex,2}$ are the wave vectors of signal, probe and of the two excitation pulses, respectively.

2. – EUV/soft x-ray transient grating experiments: the TIMER project

The TIMER project represents the first step towards the development of wave-mixing methods at the FERMI [30]. The main aim of this project is the realization of a user-dedicated instrument (located at the Elastic and Inelastic Scattering (EIS) beamline) to perform transient grating (TG) experiments in the EUV/soft x-ray spectral range [31]. The TG method is based on a four-wave-mixing (FWM([1])) process in which two non-collinear coherent pulses (pump) of wavelength λ_{ex} are crossed onto the sample (see fig. 1a). The interference between these pulses generates a transient electromagnetic standing wave with spatial periodicity $L = \lambda_{ex}/(2\sin(\theta/2))$, where θ is the crossing angle between the pump beams. Such a standing wave imposes a modulation of sample parameters. For instance, it can induce gratings of electronic [32], spin [13] and molecular excitations (such as rotations or vibrations) [8]. Temperature, density and pressure modulations are also induced through optical absorption and electrostriction processes, which give rise to stimulated thermal and Brillouin scattering [7,8].

In TG experiments the various excitations that may arise from non-linear interactions are characterized by the same spatial periodicity (L), which can be experimentally set by choosing λ_{ex} and θ. One can hence define a characteristic wave vector, $Q = 2\pi/L = (4\pi/\lambda_{ex})\sin(\theta/2)$, which imposes a Q-selection rule. This allows TG to select a given mode in the Q-dispersions of collective excitations (phonons [7, 8], spin waves [13], polarons [33], etc.) or a given Fourier component of single-particle processes, such as electron or molecular diffusion [32, 15]. The time evolution of the excited modes can be determined through the FWM process by sending into the sample a third coherent pulse (probe) in phase matching conditions and by looking at the intensity of the phase-matched FWM signal as a function of the pump-probe delay (see fig. 1a). We also

---

([1]) It is worth noticing that the FWM process is the lowest order non-linear effect in systems with inversion symmetry [1], as disordered systems, which are the samples of primary interest for the TIMER project.

note that in TG experiments the phase matching conditions reduces to the Bragg law, as shown in fig. 1b. Moreover, by acting on the polarization of both pump and probe beams it is possible to disentangle spin, rotational and translational (both longitudinal and transverse) dynamics.

Nowadays, the maximum Q-range exploitable by optical TG is limited to $\approx 0.01\,\mathrm{nm}^{-1}$ by the long wavelength ($> 400\,\mathrm{nm}$) of optical photons. Picoacustic methods [34] and optical inelastic scattering techniques that exploit UV radiation (either from lasers [35, 36] or synchrotrons [37]) can probe Q-values smaller than $\approx 0.1\,\mathrm{nm}^{-1}$. On other hand, high-resolution inelastic hard x-ray scattering cannot probe Q-values lower that ≈ 1–$2\,\mathrm{nm}^{-1}$, while thermal neutron scattering is intrinsically limited by kinematic constraints. The latter prevent the study of dynamics faster than a few ps at Q-values lower than a few nm. The use of EUV/soft x-ray coherent sources tunable in both wavelength and polarization, as FERMI, would allow to probe the aforementioned dynamics in the unexplored Q-range in between $0.1\,\mathrm{nm}^{-1}$ and $1\,\mathrm{nm}^{-1}$. Indeed, the optical layout of the TG setup at EIS-TIMER is conceived to operate at λ_{ex} values as short as $10\,\mathrm{nm}$ (extendable down to $4\,\mathrm{nm}$) and at θ values as large as $106°$, thus allowing to exploit the 0.03-$1\,\mathrm{nm}^{-1}$ Q-range; stretchable up to $2.5\,\mathrm{nm}^{-1}$ for $\lambda_{ex} = 4\,\mathrm{nm}$ [30, 31, 38]. EIS-TIMER will exploit the third harmonic of the FEL emission as probe beam (*i.e.*, $\lambda_{probe} = \lambda_{ex}/3$), which allows to fulfil the phase matching constraint for all exploitable (λ_{ex}, θ)-values. A delay line consisting of multilayer mirrors working at $45°$ angle of incidence will be used to vary the pump-probe delay in the $-0.1 +3\,\mathrm{ns}$ range. Additionally, it will be also possible to change the time delay between the two pump pulses in the $-3 +7\,\mathrm{ps}$ range in order to carry out photon echo experiments [16, 39]. Two further beamlines for optical lasers ($\lambda_{opt} \approx 230$–$900\,\mathrm{nm}$) to be used either as an alternative probe and/or an additional pump will be also available. The distinguishing feature of the EIS-TIMER optical layout is the absence of transmissive optic and, in particular, transmission diffractive elements, such as phase masks, that greatly simplify optical TG experiments. This choice was forced by the fact that, at present, in the EUV/soft x-ray spectral range these elements cannot provide the necessary photon throughput and are limited in the working wavelength range. We positively tested this special layout through both ray-tracing simulations [38] and TG experiments carried out in the optical domain [40]. The experimental end-station has been realized and commissioned, while the installation of the beamline will start by the end of 2015.

The main scientific aim of EIS-TIMER is the study of collective atomic dynamics in disordered systems, such as glasses or liquids, in the presently unaccessible "mesoscopic" Q-range (0.1–$1\,\mathrm{nm}^{-1}$) [31]. In these systems the lack of translational invariance leads to other characteristic lengthscales ($\xi \approx 10\,\mathrm{nm}$) related to the topological disorder and to local molecular structures. The presence of these length scales is believed to greatly affect the dynamics at the molecular scale, as well as the thermal and mechanical behavior at the macroscopic level [41-44]. Furthermore, numerous dynamical processes characterized by different timescales (*e.g.*: relaxations, hopping, anharmonic interactions, intramolecular modes, etc.) can couple with collective excitations in specific Q-ranges, thus contributing to the peculiar thermal and mechanical behavior of disordered systems as compared to crystalline solids [45]. The interplay between structural and dynamical scales prevented the development of a exhaustive and commonly accepted framework to describe the dynamics of disordered systems at such "mesoscopic" scale, even though theoretical and experimental works suggest that this scale is the one that plays the major role in the determination of the macroscopic properties of disordered systems [41-44, 46-48].
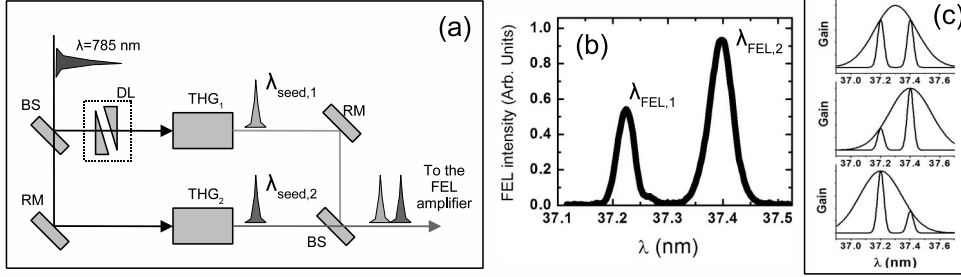
Fig. 2. – (a) Optical system used to obtain the two seed laser pulses: BS, RM, THG$_{1,2}$ and DL are 50:50 beamsplitters, reflective mirrors, third-harmonic generation crystals and the delay line, respectively. (b) Wavelength spectrum of the two-color FEL emission, as measured by a EUV/soft x-ray spectrometer. The area of each of the two spectral lines is proportional to the energy per pulse of the corresponding spectral component ($\approx 10\,\mu$J in the present case). (c) Changes in the relative intensity between the two-color pulses as a function of the wavelength shift of the FEL gain bandwidth; the double-peak structure represents the FEL spectrum (as in panel b).

3. – Multi-color, fully coherent FEL pulses at FERMI: a step towards FWM experiments

Several wave-mixing methods require multi-color excitation and probe pulses, as well as the possibility to change the wavelength difference among them [49]. The option to use the harmonics of the FEL emission cannot completely fulfil this requirement, since the wavelengths cannot be separately set. In the quest to overcome this limitation we recently demonstrated the possibility to use multiple independent seed laser pulses to obtain a multi-pulse and multi-color FEL emission with independent control of relative intensity, wavelength difference and time separation of the two pulses [29]. In particular, as shown in fig. 2a, we split the output of a Ti:sapphire laser ($\lambda = 785$ nm) into two independent optical paths, each equipped with third harmonic generation crystals able to provide independent wavelength tunability in the 260–262 nm range. One of the two pulses is time delayed with respect to the other by an optical delay line, consisting of two wedged slabs, and then recombined in a single beamline. The output of this simple optical setup is a train of two-color collinear pulses of wavelength $\lambda_{seed,1}$ and $\lambda_{seed,2}$, that can be sent into the FEL amplifier. As long as $\lambda_{seed,1}$ and $\lambda_{seed,2}$ are within the gain bandwidth of the FEL radiators, both pulses are amplified and give rise to a double FEL emission at $\lambda_{FEL,1} = \lambda_{seed,1}/H$ and $\lambda_{FEL,2} = \lambda_{seed,2}/H$ (see fig. 2b). The central wavelength, bandwidth and time duration of both pulses, as well as their time separation, can be independently controlled by acting on the seed pulses, while the relative intensity can be set by shifting the gain bandwidth of the radiators, as shown in fig. 2c. Finally, the two FEL pulses are expected to be coherently coupled since they arose from the same laser pulse, though we did not yet carried out experiments to demonstrate that. Further details on the experimental methodology and on the obtained results are reported elsewhere [29].

A straightforward application of such a two-color FEL radiation is represented by EUV/x-ray coherent Raman scattering (CRS) [1, 2], a FWM-based technique widely used in the optical domain to study ultrafast molecular dynamics. Similarly to TG
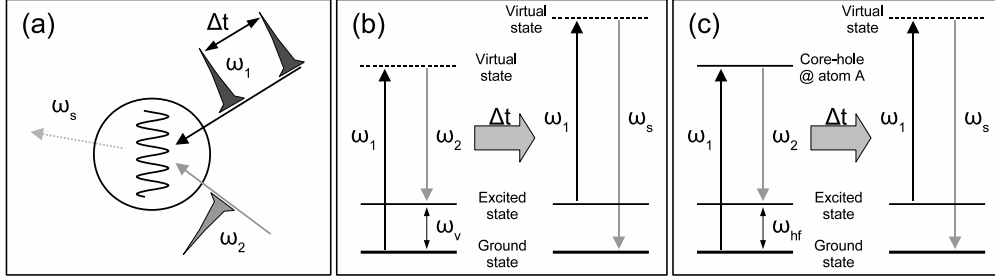
Fig. 3. – Sketch (panel a) and energy level scheme (panel b) of a typical optical CRS experiment. (c) Energy level scheme of an EUV/x-ray CRS experiment involving a core transition in the excitation process; see text for further details.

experiments, in CRS the two pump pulses are crossed into the sample in time and space coincident conditions. Differently from TG, the exciting pulses do not have the same photon frequency (*i.e.*, the same color). If $(\omega_1, \vec{k}_1)$ and $(\omega_2, \vec{k}_2)$ are the field frequencies and wavevectors of pump beams, then the standing electromagnetic wave (of spatial periodicity $L = 2\pi/|\vec{k}_1 - \vec{k}_2|$) has beatings at the sum and difference frequency, $\omega_1 + \omega_2$ and $\omega_1 - \omega_2$. The latter can be used to excite, *e.g.*, molecular vibrational modes at frequency $\omega_s = \omega_1 - \omega_2$. The time evolution of the stimulated excitation can be determined through the so-called coherent anti-Stokes Raman scattering process. This arises from the non-linear interaction between the excitation pulses and another $(\omega_1, \vec{k}_1)$-pulse (probe) that impinges onto the sample after a given time delayed Δt and originates the FWM (signal) field having $\omega_s = 2\omega_1 - \omega_2$ and $\vec{k}_s = 2\vec{k}_1 - \vec{k}_2$; see figs. 3a-3b.

In optical CRS the input fields frequencies are lower than $\approx 3\,\text{eV}$. Therefore, the $\omega_2 - \omega_1$ values are in the sub-eV range. This permits to study ultrafast dynamics of low-energy excitations, such as molecular vibrations or low-energy electronic excitations. Conversely, in EUV/x-ray CRS the input fields frequencies can be in the $100\,\text{eV}$ range or even much larger, so that $\omega_1 - \omega_2$ can be as large as several eV. Such a wider range in $\omega_1 - \omega_2$ can be used to study ultrafast dynamics of high energy "optical" excitations as, *e.g.*, valence band excitons [50]. Furthermore, atomic selectivity can be achieved by tuning the input fields frequencies to core transitions of given atoms. For instance, an ultrafast EUV/x-ray field (ω_1) can be used to stimulate a core transition at a selected atom A within a molecular solid, while the concurrent action of the second field (ω_2) generates the excitation at $\omega_{hf} = \omega_1 - \omega_2$; see fig. 3c. In this case the virtual state in the left hand side of fig. 3b is replaced by a real excited electronic state. Atomic selectivity is achieved thanks to the localization of core shells, that ensures that the stimulated excitation is initially centered on atom A. Atomic selectivity in the probe process can be also achieved by tuning the probe frequency (ω_3) to a core resonance of atom B [50-52]. If A and B are different atoms, then the eventual detection of a FWM signal at $\omega_s = \omega_3 - \omega_2 + \omega_1$ and $\vec{k}_s = \vec{k}_3 - \vec{k}_2 + \vec{k}_1$ provides information on the propagation of the selected excitation between the two atoms. This capability will allow to study, *e.g.*, ultrafast charge and energy transfer processes at the molecular scale with atomic selectivity.

It is worth stressing that photons arising from linear interactions (such as scattering and absorption) between each of the input fields and the sample would affect the detection of the non-linear signal of interest. The total amount of such a background signal from

linear processes can exceed the non-linear one by orders of magnitude, in particular for $E \ll E_a$ (we recall that $\chi \sim 1$ while $\chi^{(3)} \sim E_a^{-2}$ [1,5]). However, the phase matching constraint ensures that the FWM signal propagates along the $\vec{k}_s$ direction while linear interactions in the EUV/soft x-ray range result in (typically isotropic) scattering and emission processes. Therefore, the gain in the non-linear/linear signal ratio within the solid angle ($\Delta\Omega$) under which the wave-mixing signal propagates can be very large. For instance, for a typical beam divergence of $\approx 1\,\mathrm{mrad}$, one has $\Delta\Omega \approx 10^{-7}\,\mathrm{sr}$ and thus a gain $\sim 4\pi/\Delta\Omega \approx 10^8$; in ref. [52] we report a quantitative estimate of the linear *vs.* non-linear signals in a representative EUV/soft x-ray FWM experiment. Furthermore, the strong photo-ionization occurring in the EUV/soft x-ray range will ineluctably lead, *e.g.*, to distributions of excited electrons, that follow the spatial modulation imposed by the interfering beams. The relaxation dynamics of such electronic excitations can thus give rise to a FWM signal and might modify the properties of the sample. The interplay between the dynamics of the selected excitation (schematized in fig. 3c) and that of the excited electrons (and holes) will be the subject of thoroughly investigations.

Possible applications of EUV/x-ray wave mixing methods have been theoretically discussed in many details [50,53-56] and pioneering experimental works, still carried out with the assistance of optical lasers, demonstrated the occurrence of basic wave-mixing processes in the EUV [57] and x-ray ranges [58]. On such grounds we recently discussed on the scientific aims and practical implementation of EUV/x-ray FWM methods at the FERMI FEL facility [51,52]. There we showed that a substantial improvement of the FERMI source and of the optical transport system is needed in order to perform an "ideal" EUV/soft x-ray FWM experiment, that includes few-fs time-resolution as well as independent polarization and atomic selectivity in both pump and probe processes. However, the combination of the multi-color multi-pulse FEL emission([2]) and the EIS-TIMER beamline (soon available at FERMI) would allow to carry out EUV/soft x-ray FWM experiments with a few 10s of fs time resolution and atomic selectivity in the pump process [59], as sketched in fig. 3c. Though the exploitable ω_{hf} range is presently limited to below $\approx 1\,\mathrm{eV}$ by the finite bandwidth of the FEL gain curve, ω_{hf} values of about twice will likely be achievable in the near future [59].

4. – Conclusions

We reported on the development of EUV/x-ray wave-mixing spectroscopy at the FERMI facility (Trieste, Italy), which includes the realization of a user-dedicated beamline (EIS-TIMER). These techniques will fully exploit the unique coherence properties of the seeded FEL source available at the facility. Among possible wave-mixing methods, the transient grating technique will be used to study collective atomic dynamics in disordered systems in the "mesoscopic" Q-range of 0.1–$1\,\mathrm{nm}^{-1}$, not accessible by available methods. EUV/x-ray transient grating experiments are of potential great relevance also for the study of dynamical processes in nanostructures and correlated systems. The recent demonstration of the multi-pulse multi-color seeded FEL emission with indepen-

---

([2]) In ref. [29] we demonstrated a double (two-color) FEL emission. However, the number of FEL pulses within a single shot only depends on how many seeding pulses can be accomodated on the same electron bunch. Since the time duration of the latter is $\approx 1\,\mathrm{ps}$ while that of a typical seed laser pulse is ≈ 0.1–$0.2\,\mathrm{ps}$, more than two seeding pulses (eventually with more than two colors) can then be brought into interaction with the same electron bunch.

dent wavelength tunability opened up bright perspectives for the development of more advanced non-linear wave-mixing spectroscopies. In particular, EIS-TIMER is expected to allow EUV/x-ray coherent Raman scattering experiments with time resolution of a few 10's of fs and atomic selectivity in the excitation process. The latter capability is not achievable by optical methods. Although this novel experimental tool will be initially limited to the study of low-energy (sub-eV) excitations, the ongoing development of the FERMI FEL sources towards more flexible multi-pulse and multi-color operation modes would soon allow for more sophisticated wave-mixing experiments.

* * *

REFERENCES

[1] Boyd R., *Nonlinear Optics* (Elsevier, Oxford) 2008.
[2] Mukamel S., *Principles of Nonlinear Optical Spectroscopy* (Oxford University Press, Oxford) 1995.
[3] Maiman T. H., *Nature*, **187** (1960) 493.
[4] Frenken P. A, Hill A. E., Peters C. W. and Weinreich G., *Phys. Rev. Lett.*, **7** (1961) 118.
[5] Armstrong J. A., Bloembergen N., Ducuing J. and Pershan P. S., *Phys. Rev.*, **127** (1962) 1918.
[6] Giordmaine J. A., *Phys. Rev. Lett.*, **8** (1962) 19.
[7] Yan J.-X., Gamble E. B. jr. and Nelson K. A., *J. Chem. Phys.*, **83** (1985) 5391.
[8] Dhar L., Rogers J. A. and Nelson K. A., *Chem. Rev.*, **94** (1994) 157.
[9] Wörner H. J. *et al.*, *Nature*, **466** (2010) 604.
[10] Foster M. A. *et al.*, *Nature*, **441** (2006) 960.
[11] Li X. *et al.*, *Phys. Rev. Lett.*, **94** (2005) 053601.
[12] Kim H. *et al.*, *Opt. Express*, **20** (2012) 6042.
[13] Cameron A. R., Riblet P. and Miller A., *Phys. Rev. Lett.*, **76** (1996) 4793.
[14] Morishita T. *et al.*, *J. Phys. Chem. B*, **103** (1999) 5984.
[15] Terazima M., Okamoto K. and Hirota N., *J. Phys. Chem.*, **97** (1993) 5188.
[16] Nibbering E. T. J., Wiersma D. A. and Duppen K., *Phys. Rev. Lett.*, **66** (1991) 2464.
[17] Dhar L. and Rogers J. A., *Appl. Phys. Lett.*, **77** (2000) 1402.
[18] Banet M. J. *et al.*, *Appl. Phys. Lett.*, **73** (1998) 169.
[19] Mairesse Y. *et al.*, *Phys. Rev. Lett.*, **100** (1998) 143903.
[20] Bressler C. *et al.*, *Science*, **323** (2009) 489.
[21] Vankó G. *et al.*, *Angew. Chem., Int. Ed.*, **49** (2010) 5910.
[22] Cammarata M. *et al.*, *Nature Methods*, **5** (2008) 881.
[23] Gallmann L., Cirelli C. and Keller U., *Annu. Rev. Phys. Chem.*, **63** (2012) 447.
[24] Singer A. *et al.*, *Phys. Rev. Lett.*, **101** (2008) 254801.
[25] http://www.elettra.trieste.it/lightsources/fermi.html.
[26] Doyuran A. *et al.*, *Phys. Rev. Lett.*, **86** (2001) 5902.
[27] Allaria E. *et al.*, *Nat. Photon.*, **6** (2012) 699.
[28] Allaria E. *et al.*, *New J. Phys.*, **14** (2012) 113009.
[29] E. Allaria *et al.*, *Nat. Commun.*, **4** (2013) 2476.
[30] http://www.elettra.trieste.it/lightsources/fermi/fermi-beamlines/eis/eis-home.html.
[31] Bencivenga F. and Masciovecchio C., *Nucl. Instrum. Methods A*, **606** (2009) 785.
[32] Sjodin T., Petek H. and Dai H.-L., *Phys. Rev. Lett.*, **81** (1998) 5664.

[33] DOUGHERTY T. P., WIEDERRECHT G. P. and NELSON K. A., *J. Opt. Soc. Am. B*, **9** (1992) 2179.

[34] PONTECORVO E. *et al.*, *Appl. Phys. Lett.*, **98** (2011) 011901.

[35] BENASSI P. *et al.*, *Rev. Sci. Instrum.*, **76** (2005) 013904.

[36] BENCIVENGA F. *et al.*, *Rev. Sci. Instrum.*, **83** (2012) 103102.

[37] MASCIOVECCHIO C., BENCIVENGA F. and GESSINI A., *Cond. Matt. Phys.*, **11** (2008) 47.

[38] CUCINI R., BENCIVENGA F., ZANGRANDO M. and MASCIOVECCHIO C., *Nucl. Instrum. Methods A*, **635** (2011) S69.

[39] FOURKAS J. T., KAWASHIMA H. and NELSON K. A., *J. Chem. Phys.*, **103** (1995) 4393.

[40] CUCINI R., BENCIVENGA F. and MASCIOVECCHIO C., *Opt. Lett.*, **36** (2011) 1032.

[41] SCHIRMACHER W., *Europhys. Lett.*, **73** (2006) 892.

[42] SCHIRMACHER W., RUOCCO G. and SCOPIGNO T., *Phys. Rev. Lett.*, **98** (2007) 025501.

[43] MASCIOVECCHIO C. *et al.*, *Phys. Rev. Lett.*, **97** (2006) 035501.

[44] FERRANTE C. *et al.*, *Nat. Commun.*, **4** (2013) 1793.

[45] PHILLIPS W. A. (Editor), *Amorphous Solids: Low-Temperature Properties* (Springer-Verlag, Berlin) 1981.

[46] SCHIRMACHER W., *Phys. Status Solidi C*, **5** (2008) 862.

[47] FABIAN J. and ALLEN P. B., *Phys. Rev. Lett.*, **82** (1999) 1478.

[48] BINDER K. and KOB W., *Glassy Materials and Disordered Solids: An Introduction* (World Scientific, London) 2011.

[49] BLOEMBERGEN N., *Recent Progress in Four-Wave Mixing Spectroscopy*, in *Laser Spectroscopy IV*, edited by WALTHER H. and ROTHE K. W. (Springer, Berlin) 1979.

[50] TANAKA S. and MUKAMEL S., *Phys. Rev. Lett.*, **89** (2002) 043001.

[51] BENCIVENGA F. *et al.*, *Proc. SPIE*, **8778** (2013) 877807.

[52] BENCIVENGA F. *et al.*, *New J. Phys.*, **15** (2013) 123023.

[53] TANAKA S. *et al.*, *Phys. Rev. A*, **63** (2001) 063405.

[54] TANAKA S. and MUKAMEL S., *J. Chem. Phys.*, **116** (2002) 1877.

[55] MUKAMEL S., *Phys. Rev. B*, **72** (2005) 235110.

[56] PATTERSON B. D., *SLAC Technical Note*, **SLAC-TN-10-026** (2010) .

[57] MISOGUTI L. *et al.*, *Phys. Rev. A*, **72** (2005) 063803.

[58] LUTMAN A. A. *et al.*, *Phys. Rev. Lett.*, **110** (2013) 134801.

[59] BENCIVENGA F. *et al.*, *Faraday Discuss.* (2014) DOI:10.1039/C4FD00100A.